



# Equilibrium shape of rotating helium crystals

A.Ya. Parshin

*P.L. Kapitza Institute for Physical Problems, Russian Academy of Sciences, 117334 Moscow, Russian Federation*

## Abstract

We have studied theoretically the effects of rotation on the equilibrium shape of the interface between superfluid and solid helium. Surface structures in the shape of hillocks and ridges appear in the presence of a vortex lattice in the superfluid. These structures are very sensitive to the orientation of the interface boundary with respect to the crystal planes when surface stiffness is very anisotropic, as occurs well below the roughening transition. We predict the appearance of ring shaped facets for fast rotation speeds. These effects should be observable by using optical techniques.

## 1. Introduction

It is well known that vortex lines in rotating superfluid helium with a free surface alter the shape of the surface—they form small dimples of about  $60 \text{ \AA}$  in height [1]. Similar dimples appear at the interface separating a superfluid from another liquid or gas [2]. In the case of the solid-superfluid helium interface one also expects this phenomenon, but with bulges instead of dimples: bulges because the superfluid is the lighter phase so it floats on the surface of the solid.

Usually the dimples or bulges are too small to be seen directly even with modern optical technique [3, 4]. The main limiting factor is the surface tension,  $\alpha$ , which has the same order of magnitude for the solid-liquid and liquid-vapor interfaces. However in crystals, as in any anisotropic medium, the quantity which controls the surface curvature is the tensor of surface stiffness. In hcp  $^4\text{He}$  crystals the principal components of this tensor are known to depend strongly on the surface orientation [5, 6]; in particular one component becomes very small in the vicinity of the basal plane (0001) at low temperature. As a consequence the structures formed by the vortices in this special case are quite different, and more importantly, the size of the structures is much larger than in the case of an arbitrary surface orientation. Under

some circumstances the forms of hillocks and ridges are large enough to be observed optically. In this paper we explore the conditions where this occurs.

Apart from the hillocks we predict a new effect for the global shape of the rotating crystal. Consider a crystal with a horizontal basal plane rotating in a cylindrical vessel. If the interface is rough the global shape would be a parabola. When the interface is faceted the free energy in the rotating frame is minimized with a different shape in which there is a central facet (0001) and a circular concentric facet separated by a section of curved surface. This effect only happens above a critical angular velocity of rotation. This effect can also be observed optically.

## 2. Basic equations and experimental data on the surface tension anisotropy

We consider the following experimental set-up (Fig. 1): a cylindrical vessel with vertical axis, rotating around it with angular velocity  $\Omega$ , containing a crystal of  $^4\text{He}$  in equilibrium with liquid phase,  $c$ -axis of the crystal being tilted by an angle  $\tau$ . We have to study the interface boundary profile  $z = \zeta(x, y)$ , taking into account the motion of a liquid due to the presence of vortices. In a macroscopical approach this profile can be found from



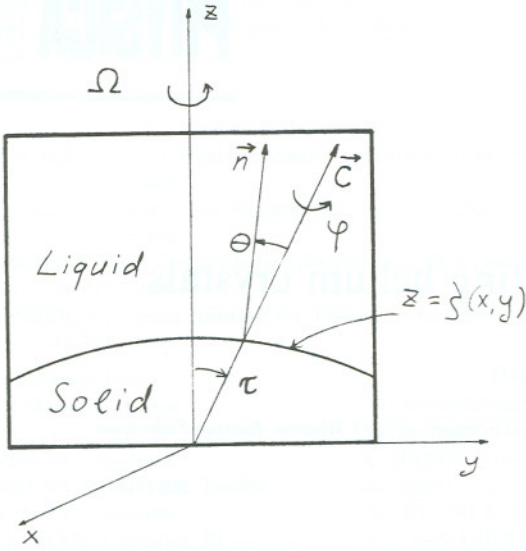


Fig. 1. Typical experimental arrangement.

the condition of phase equilibrium for rotating media. In the case of slow motion, when characteristic velocities are much less than the velocity of sound, we can neglect the dependence of  $\alpha$  on the relative velocity ( $\mathbf{v}_l - \mathbf{v}_s$ ) and write (see Refs. [7, 8]):

$$\left(\frac{1}{\rho_l} - \frac{1}{\rho_s}\right)\delta p_l + \frac{1}{\rho_s} f''_{\mu\nu} \zeta''_{\mu\nu} + \frac{1}{2}(\mathbf{v}_l - \mathbf{v}_s)^2 = 0 \quad (1)$$

where  $l$  and  $s$  indicate liquid and solid, respectively ( $\mathbf{v}_l$  is the velocity of superfluid component),  $\delta p_l = p_l - p_0$  is the liquid pressure, measured from the nominal equilibrium pressure of a flat interface in absence of any flows,

$$f = \alpha(\theta, \phi) \sqrt{1 + \zeta''_{\mu}{}^2}$$

is the surface free energy per unit area in the  $x, y$  plane,

$$\zeta'_{\mu} = \frac{\partial \zeta}{\partial x_{\mu}}, \quad f''_{\mu\nu} = \frac{\partial^2 f}{\partial \zeta'_{\mu} \partial \zeta'_{\nu}}, \quad \mu, \nu = x, y,$$

$\theta$  and  $\phi$  being, respectively, colatitude and the longitude angle of the interface normal  $\mathbf{n}$  with respect to  $c$ -axis, which dependencies on  $\tau$  and  $\zeta'_{\mu}$  in general case are given by formulas of spherical trigonometry (we assume that  $c$ -axis tilted in  $x$ -direction):

$$\cos \theta = \frac{\cos \tau - \zeta'_x \sin \tau}{\sqrt{1 + \zeta''_{\mu}{}^2}}, \quad (2a)$$

$$\sin \phi = -\frac{\zeta'_y}{\sin \theta \sqrt{1 + \zeta''_{\mu}{}^2}}. \quad (2b)$$

Note that if  $\alpha = \text{const.}$ , the term  $f''_{\mu\nu} \zeta''_{\mu\nu}$  take the usual form of Laplace pressure  $\alpha(1/R_1 + 1/R_2)$ .

For the following analysis we need to specify the dependence of  $\alpha$  on  $\theta$  and  $\phi$  in the case of small  $\theta$ ,  $\theta \leq 0.01$ . Experimental data [5, 6] show that in this case  $\alpha$  practically does not depend on  $\phi$ . As for the dependence  $\alpha(\theta)$ , at small  $\theta$  and low temperatures it's resonable to use the model of stepped surface (see for a review Ref. [9]), which yields ( $t = \tan \theta$ )

$$\alpha(\theta) \sqrt{1 + t^2} = \alpha_0 + \beta t + \frac{\gamma}{6} t^3 + O(t^4), \quad (3)$$

where  $\alpha_0$  is the surface tension of the basal plane,  $\beta a$  is the free energy per unit length of the elementary step,  $a$  is its height,  $\gamma$  is a parameter of step-step interaction,  $\beta$  and  $\gamma$  both are essentially temperature dependent. Using Eqs. (2a) and (3) one can calculate the components of the surface stiffness tensor in the limit of small  $\theta$ . In particular, for a horizontal interface ( $\zeta'_{\mu} = 0, \theta = \tau$ ) we have

$$f_{xx} = \gamma \tau, \quad f_{yy} = \frac{\beta}{\tau}, \quad f_{xy} = 0, \quad (4)$$

i.e. well-known expressions for longitudinal ( $f_{xx}$ ) and transversal ( $f_{yy}$ ) surface stiffnesses;  $f_{yy} \gg f_{xx}$  in this limit. It is necessary to note that experimental data on  $\beta$  and  $\gamma$  are rather controversial (see Refs. [5, 6]); moreover, the latest data obtained by Rolley et al. [10] show that at low temperatures  $\gamma$  is very small and the next term in the expansion (3) dominate at  $\theta \sim 0.01$ . From theoretical point of view, Andreev [11] criticized the model of stepped surface and concluded that strictly speaking the very form of this expansion is incorrect at any nonzero temperature. However, at low temperatures (0.1 K or lower) Andreev's arguments seem to be valid only at very large scales. Taking into account all these issues, we will use the expansion (3) in our analysis. For numerical estimations we assume: at  $T \leq 0.1\text{K}$   $\beta \approx 0.01 \text{ erg/cm}^2$ ,  $\gamma \approx 0.5 \text{ erg/cm}^2$  (see Ref. [6]).

In the following analysis we assume also that  $\zeta'_{\mu}$  are continuous function of  $x, y$  everywhere on the interface (with only one possible exception of end points of vortex cores, which should be considered in a macroscopical approach as singular points). This assumption is equivalent to the condition of local stability of any surface orientation, at least in the vicinity of basal plane (0001). It means that  $f''_{\mu\nu}$  is a positive-definite matrix for any small  $\theta$ . As far as we know, all experimental data on the equilibrium shape of helium crystals support this assumption (see e.g. Ref. [12]). In our approximation the presence of superflow does not change the surface tension and hence does not lead to the surface instability of this type. One can say that in this work an another type of



instability is considered, similar to the Kelvin–Helmholtz type (see Ref. [7]).

### 3. Hillock on the basal plane formed by a single vortex

Consider at first a crystal with zero tilt angle  $\tau$ . In this case we have a facet (0001) in the center of the cell and an array of vortex lines normal to the facet. In the liquid bulk these vortices form a triangular lattice with the distance between nearest neighbors  $b = [2\pi\hbar/\sqrt{3}m\Omega]^{1/2}$  where  $\hbar$  is the Planck constant,  $m$  is mass of  $^4\text{He}$  atom (see for a review Ref. [13]). This lattice rotate as a solid with the same angular velocity  $\Omega$ , and we can assume that it remains underformed down to the crystal surface. Let  $\mathbf{R}_i$  be the position of one of the vortices axis. At small distances  $r \ll b$ ,  $\mathbf{r} = \mathbf{R} - \mathbf{R}_i$  ( $\mathbf{R}, \mathbf{R}_i$  being measured from the rotation axis),  $\mathbf{v}_\ell$  can be expressed in the form

$$\mathbf{v}_\ell = \mathbf{v}_s + \mathbf{v}_i, \quad \mathbf{v}_i = \nabla\dot{\phi} \sim \frac{\hbar}{m\Omega r^2} [\Omega \times \mathbf{r}]. \quad (5)$$

Corresponding expression for  $\delta p_\ell$  is:

$$\begin{aligned} \delta p_\ell &= -\rho_\ell(\dot{\phi} + \frac{1}{2}v_i^2) - \rho_\ell g\zeta + \text{const.} \\ &= -\frac{\rho_\ell}{2} \left(\frac{\hbar}{mr}\right)^2 - \rho_\ell g\zeta + \text{const.} \end{aligned} \quad (6)$$

(we neglect very small difference between  $\rho_i$  and the density of superfluid component; the second term in Eq. (4) is due to gravity).

With the surface tension  $\alpha$  independent on angle  $\phi$  we may expect that the minimum possible energy will have an axially symmetric bulge, quite similar to the case of the dimple formed by an individual vortex on the surface of liquid helium ([1, 2]; see, however, Ref. [16]). Therefore, we shall look for a solution of the type of axisymmetric hillock  $\zeta(r)$  (see Fig. 2); thus we obtain from Eq. (1):

$$-\frac{1}{r} \frac{d}{dr} \left( r f_i' \right) + \frac{\rho_\ell}{2} \left(\frac{\hbar}{m}\right)^2 \frac{1}{r^2} - (\rho_s - \rho_\ell) g\zeta + \Delta = 0 \quad (7)$$

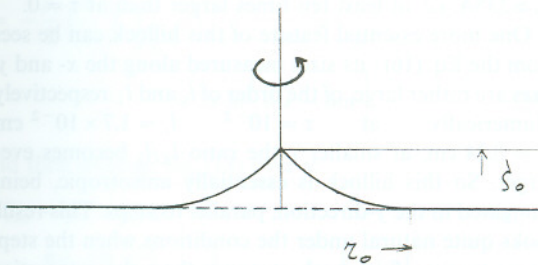


Fig. 2. A hillock on the basal plane.

for  $\zeta' = -t < 0$  (here  $t = |\zeta'|$ ); pay attention to  $\delta$ -singularity at  $\zeta' = 0$ ; here  $\Delta$  is a constant, which can be determined from the solution of Eq. (1) for the whole interface. As we shall see from the result, the gravitational term in Eq. (7) can be neglected. The first integration yields

$$f_i' = \beta + \frac{\gamma}{2} \zeta'^2 = \frac{\rho_\ell}{2} \left(\frac{\hbar}{m}\right)^2 \frac{1}{r} \ln \frac{r}{c} + \frac{\Delta}{2} r. \quad (8)$$

The constant of integration  $c$  defines the behavior of  $\zeta'$  in the limit of small  $r$ ; taking into account that our macroscopic approach becomes invalid at distances of the atomic scale  $r \sim a$ , it seems reasonable to set  $c \sim a$ . Further, we are looking for a solution, which is localized near  $r = 0$ ; in other words, must be  $\zeta' = \zeta = 0$  at  $r \rightarrow \infty$ . Eq. (8) has continuous solution of this type if  $\Delta \leq \Delta_m$ , where

$$\Delta_m \approx \beta^2 \frac{1}{\rho_\ell} \left(\frac{m}{\hbar}\right)^2 \ln^{-1} \frac{\rho_\ell \hbar^2}{\beta a m^2}. \quad (9)$$

At  $\Delta = \Delta_m$  the hillock's radius can be estimated as

$$r_0 \approx \frac{\beta}{\Delta_m} \approx \frac{\rho_\ell}{\beta} \left(\frac{\hbar}{m}\right)^2 \ln \frac{\rho_\ell \hbar^2}{\beta a m^2} \approx 115 \text{ \AA}, \quad (10)$$

and its height

$$\zeta_0 \approx \frac{4}{3} r_0 \sqrt{\frac{\beta}{\gamma}} \approx 22 \text{ \AA}. \quad (11)$$

Numerical values of  $r_0$  and  $\zeta_0$  decrease if  $\Delta$  decreases; e.g. at  $\Delta = 0$

$$r_0 \approx \frac{\rho_\ell}{2\beta} \left(\frac{\hbar}{m}\right)^2 \ln \frac{\rho_\ell \hbar^2}{2\beta a m^2} \approx 43 \text{ \AA}, \quad (12)$$

$$\zeta_0 \approx \pi r_0 \sqrt{\frac{\beta}{2\gamma}} \approx 13 \text{ \AA}.$$

Turning back to Eq. (7) we see that the gravitational term is really negligible. In the opposite case,  $\Delta > \Delta_m$ , Eq. (8) has only delocalized solutions,  $|\zeta'| \rightarrow \infty$  at  $r \rightarrow \infty$ . It means that actually such an interface is not in equilibrium, the crystal should grow under these conditions. The value of  $\Delta_m$  is thus the critical overpressure (or supercooling force, according to Nozières [9]) for the facet growth in the presence of vortices (note that  $r = \beta/\Delta$  is the radius of critical nucleus for a given value of overpressure  $\Delta$ ).

### 4. Hillocks and terraces on vicinal interfaces

Now turn to the case of nonzero tilt angles  $\tau$ . Let again the crystal  $c$ -axis be tilted in the  $x$ -direction. A horizontal surface of such a crystal might be considered as an array of straight steps parallel to the  $y$ -axis with spacing  $d = a/\tau$ .

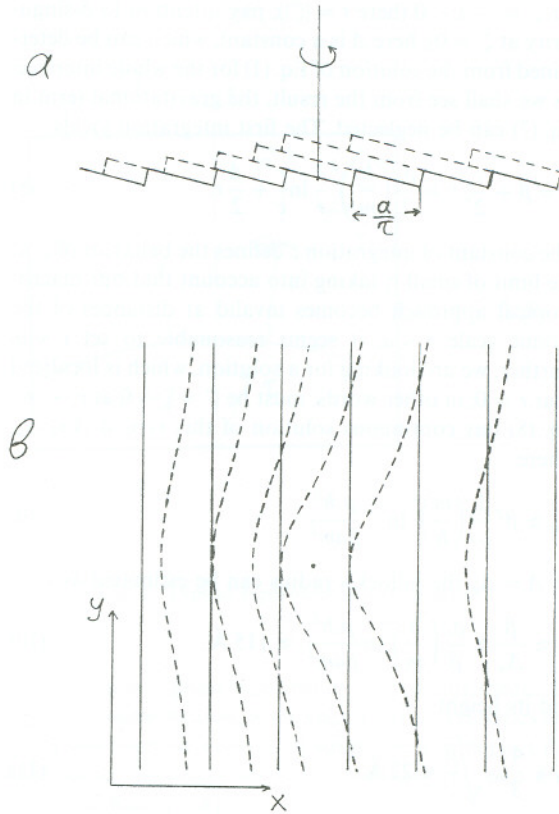


Fig. 3. Formation of a bulge as a result of displacement and bending of steps: (a)  $x$ - $z$  section, (b) top view.

At small  $\tau$ , when  $d \gg r_0$  with  $r_0$  from Eq. (10) or (12), the solution presented in the previous section is still valid, but an additional mechanism of the surface bulging appear in this case, due to displacement and binding of steps (see Fig. 3(a), 3(b)). For the same reason the value of overpressure  $\Delta$  is zero in this case.

In order to estimate the effect of step displacement, remaining in the frames of our macroscopical approach, we should come to length scales much larger than  $d$ . Corresponding differential equation is essentially nonlinear in  $\zeta''_{\mu}$  and can be solved analytically only after linearization; assuming that  $\zeta''_{\mu} \ll \tau$  and using Eq. (4), we write

$$\gamma \tau \zeta''_{xx} + \frac{\beta}{\tau} \zeta''_{yy} + \frac{\rho_l}{2} \left( \frac{\hbar}{m} \right)^2 \frac{1}{r^2} - (\rho_s - \rho_l) g \zeta = 0. \quad (13)$$

We are again looking for a localized solution, i.e.  $\zeta \rightarrow 0$  at  $r \rightarrow \infty$ . Besides that, we need one more boundary condition, concerning the behavior of  $\zeta''_{\mu}$  at  $r \rightarrow 0$  (actually, at  $r \sim d$ ). Strictly speaking, this condition can be derived only from "mesoscopical" consideration of the equations of steps equilibrium. However, the underlying physics is

clear. The equilibrium condition for the "last" step, at  $r \sim d$  includes the driving force by the central region of the vortex. We may allow for this driving force macroscopically just introducing in the right hand of Eq. (13) a "source" in the form of  $\delta$ -function with the amplitude  $A$  equal to the integral action of the central region:

$$A = \int_a^d \frac{\rho_l}{2} \left( \frac{\hbar}{m} \right)^2 \frac{1}{r^2} 2\pi r dr = \pi \rho_l \left( \frac{\hbar}{m} \right)^2 \ln \frac{1}{\tau}. \quad (14)$$

After that, in order to find the desired solution, it is convenient to include the point  $r = 0$  with its vicinity in the domain of Eq. (13). To do it we only need to replace the singular term  $1/r^2$  by a function which is smooth in the scale  $r \sim d$ , e.g.  $1/(r^2 + d^2)$ ; as a result, the solution remains correct with logarithmic accuracy. We have finally

$$\gamma \tau \zeta''_{xx} + \frac{\beta}{\tau} \zeta''_{yy} - g(\rho_s - \rho_l) \zeta = - \frac{\rho_l}{2} \left( \frac{\hbar}{m} \right)^2 \frac{1}{r^2 + d^2} - A \delta(r). \quad (15)$$

Now, using  $2d$  Fourier transformation, we obtain the solution of Eq. (15) in the form

$$\begin{aligned} \zeta(r, \psi) = & \frac{A}{2\pi \sqrt{\beta \gamma}} K_0 \left( r \sqrt{\left( \frac{\cos \psi}{l_{\parallel}} \right)^2 + \left( \frac{\sin \psi}{l_{\perp}} \right)^2} \right) \\ & + \frac{\rho_l}{4\pi(\rho_s - \rho_l)g} \left( \frac{\hbar}{m} \right)^2 \int_0^{\infty} k dk \\ & \times \int_0^{2\pi} d\omega \frac{K_0(kd) e^{ikr \cos(\omega - \psi)}}{k^2(l_{\parallel}^2 \cos^2 \omega + l_{\perp}^2 \sin^2 \omega) + 1}, \end{aligned} \quad (16)$$

where  $\tan \psi = y/x$ ,  $K_0$  is the McDonald's function,  $l_{\parallel} = \sqrt{\gamma \tau / (\rho_s - \rho_l) g}$  and  $l_{\perp} = \sqrt{\beta / (\rho_s - \rho_l) g \tau}$  — the capillary lengths in  $x$ - and  $y$ - direction, respectively,  $l_{\perp}$  being much larger than  $l_{\parallel}$ . For the height of this hillock  $\zeta_0$  at  $r \sim d$  we find from Eq. (16),

$$\zeta_0 \approx \frac{\rho_l}{4} \frac{1}{\sqrt{\beta \gamma}} \left( \frac{\hbar}{m} \right)^2 \ln \frac{\tau l_{\parallel}}{a} \ln \frac{l_{\parallel}}{\tau a}. \quad (17)$$

The numerical estimation of Eq. (17) at  $\tau \sim 10^{-2}$  yields  $\zeta_0 \approx 235 \text{ \AA}$ , i.e. at least ten times larger than at  $\tau = 0$ .

One more essential feature of this hillock can be seen from the Eq. (16): its sizes measured along the  $x$ - and  $y$ - axes are rather large, of the order of  $l_{\parallel}$  and  $l_{\perp}$  respectively. Numerically, at  $\tau = 10^{-2}$   $l_{\parallel} = 1.7 \times 10^{-2}$  cm,  $l_{\perp} = 0.24$  cm; at smaller  $\tau$  the ratio  $l_{\perp}/l_{\parallel}$  becomes even larger. So this hillock is essentially anisotropic, being elongated in the  $y$ -direction, parallel to steps. This result looks quite natural under the conditions when the steps linear tension  $\beta$  is much stronger than the interaction between them  $\gamma \tau^2$ .



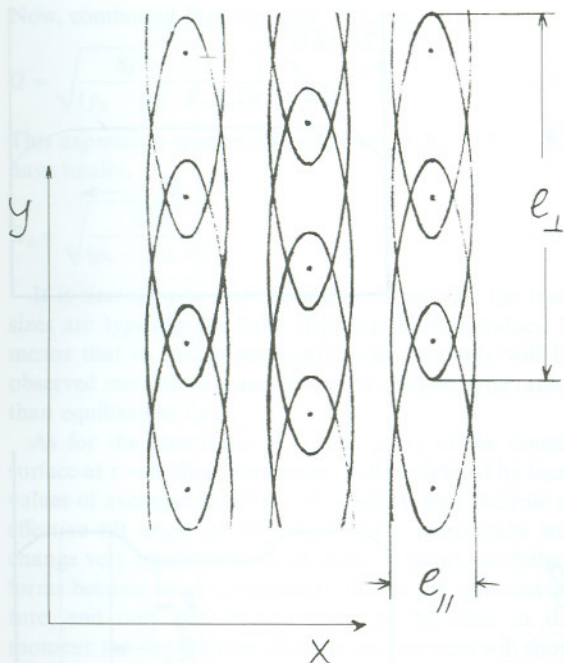


Fig. 4. Ridges on a vicinal surface formed by a vortex lattice.

Now let us take into account the existence of vortex lattice in rotating superfluid. The lattice parameter  $b$  can be, depending on  $\Omega$ , larger or shorter than  $l_{||}$ ,  $l_{\perp}$  (e.g. at  $\Omega = 1$  rad/s,  $b = 2.4 \times 10^{-2}$  cm). Consider the situation when  $b$  meets the condition  $l_{||} \ll b \ll l_{\perp}$ , vector  $\mathbf{b}$  directed along the  $y$ -axis. In this case the bulges which belong to one of the lattice rows parallel to  $\mathbf{b}$ , strongly overlap each other; at the same time, there is practically no overlapping between different rows (Fig. 4). Such an interface may be viewed as a regular array of well separated ridges with spacing  $\sqrt{3}b/2$ , almost homogeneous in the  $y$ -direction. In order to find the average profile of a ridge  $\zeta(x)$ , we write first

$$\begin{aligned} & \gamma\tau\zeta''_{xx} + \frac{\beta}{\tau}\zeta''_{yy} - (\rho_s - \rho_l)g\zeta \\ &= -\frac{\rho_l}{2}\left(\frac{\hbar}{m}\right)^2 \sum_n \left[ \frac{1}{x^2 + (y - bn)^2 + d^2} + 2\pi \ln \frac{1}{\tau} \delta(r - bn) \right], \end{aligned} \quad (18)$$

and then average Eq. (18) over  $y$ :

$$\begin{aligned} & \gamma\tau\zeta''_{xx} - (\rho_s - \rho_l)g\zeta \\ &= -\frac{\pi\rho_l}{2b}\left(\frac{\hbar}{m}\right)^2 \left[ \frac{1}{\sqrt{x^2 + d^2}} + 2 \ln \frac{1}{\tau} \delta(x) \right]. \end{aligned} \quad (19)$$

Now, again using the Fourier transformation, we find:

$$\begin{aligned} \zeta(x) = \frac{\rho_l}{b\gamma\tau} \left(\frac{\hbar}{m}\right)^2 & \left[ \frac{\pi}{2} l_{||} \ln \frac{1}{\tau} \exp\left(-\frac{|x|}{l_{||}}\right) + \int_0^\infty \frac{K_0(kd) \cos kx dk}{k^2 + 1/l_{||}^2} \right]. \end{aligned} \quad (20)$$

In particular,

$$\zeta(0) \approx \frac{\pi}{2} \frac{\rho_l}{b\gamma\tau} \left(\frac{\hbar}{m}\right)^2 l_{||} \ln \frac{1}{a}. \quad (21)$$

As one could expect, this value approximately  $l_{||}/b$  larger than  $\zeta_0$  from Eq. (17); for example, at  $\tau = 10^{-2}$  and  $b = 2.4 \times 10^{-2}$  cm,  $\zeta(0) \approx 1300$  Å. At smaller  $\tau$  the ridge's height  $\zeta(0)$  grows up, its width  $l_{||}$  decreases, and at  $\tau \sim 10^{-3}$  the condition  $\zeta'_x \ll \tau$  turns out to be violated. It means that the linear equation (19) is no longer correct at such a small tilt angles; instead of the term  $\gamma\tau\zeta''_{xx}$  we should write  $\gamma(\tau + \zeta'_x)\zeta''_{xx}$ . An analysis of that nonlinear equation is more complicated, however one easy can see that the solution  $\zeta(x)$  loses its symmetry  $x \rightarrow -x$  and at  $\lambda = (\rho_l/b\gamma\tau^2)(\hbar/m)^2 \sim 1$  a strip of the facet  $\theta = \tau + \zeta'_x = 0$  appears on the right slope of the ridge, which will look as a terrace in this case. Note that even nonlinear macroscopical equations of that type become invalid at still smaller  $\tau$ , when  $l_{||} \sim d$ , i.e. at  $\tau \sim ((\rho_s - \rho_l)ga^2/\gamma)^{1/3} \approx 3 \times 10^{-5}$ . At such a small  $\tau$  strips with  $\theta = 0$  take almost all the surface area, and we return to the case of zero tilt.

### 5. Effects of rotation in the long-range limit: ring-shaped facets

At large scales,  $r \gg b$ , we may neglect the inhomogeneous distribution of  $\mathbf{v}_l$  near vortices and consider the superfluid as a normal liquid rotating with the same angular velocity  $\Omega$ , i.e. we may put  $\mathbf{v}_l - \mathbf{v}_c = 0$ . The pressure  $\delta p_l$  in this case is given by usual expression

$$\delta p_l = \frac{\rho_l}{2} \Omega^2 R^2 - \rho_l g \zeta. \quad (22)$$

For the surface of a tilted crystal the equilibrium equation looks therefore as

$$\gamma\tau\zeta''_{xx} + \frac{\beta}{\tau}\zeta''_{yy} + (\rho_s - \rho_l) \left( \frac{\Omega^2 R^2}{2} - g\zeta \right) = 0, \quad (23)$$

with the solution in the form of usual parabolic meniscus

$$\zeta = \zeta_0 + \frac{\Omega^2 R^2}{2g} \quad (24)$$

for the central region and more complicated form near the walls of the vessel.

Coming back to the previous section, note that the values of bulges calculated there should be measured, strictly speaking, from the meniscus (24). It means that tilt angles in Eqs. (16), (20) include the slope of this meniscus. As a result the parameters of hillocks and ridges are somewhat different at different points in line with changes of this slope. In particular, due to bending of steps on such a surface (from Eq. (24), the steps curvature  $\kappa \sim \Omega^2/g\tau$ ), the hillocks forming a ridge turn with respect to each other and eventually stop overlapping; in other words, the ridges (16), (17) have some finite length  $L$  in the  $y$ -direction, which can be estimated as  $L \sim l_y/l_1\kappa$ . Numerically, at  $\tau \sim 10^{-2}$ ,  $\Omega \sim 1$  rad/s,  $L \sim 1$  cm. For large crystals,  $R_0 \gg L$ , one can expect the appearance of ridges with different orientations in the  $x$ - $y$  plane, corresponding to different directions of the vortex lattice translation vectors. However, in order to find the shapes and distribution of ridges on the whole surface in this case we have to solve essentially two-dimensional and nonlinear equations (see also the end of this section).

More interesting picture arises for zero tilt angle. In this case the crystal surface usually consist of a circular facet  $\zeta' = 0$  in its central region and a surface in the form of convex meniscus, due to poor wetting of the vessel walls (see e.g. Ref. [14], Fig. 5(a)). Let us consider the effect of rotation on such a surface.

Instead of Eq. (7), we have now

$$\frac{1}{R} \frac{d}{dR} \left( R \frac{df}{d\zeta'} \right) + (\rho_s - \rho_l) \left( \frac{\Omega^2 R^2}{2} - g\zeta \right) = 0, \quad (25a)$$

where  $f = \alpha_0 + \beta|\zeta'| + (\gamma/6)|\zeta'|^3$ ,  $\zeta' = d\zeta/dR$ ,  $\zeta$  being measured from a reference level, which depend, in particular, on  $\Omega$ , on the total crystal volume in the vessel and on the wetting angle. It is worth also to rewrite Eq. (25a) in the form which is more convenient at  $\zeta' \neq 0$ :

$$\gamma|\zeta'| \zeta'' + \frac{\zeta'}{|\zeta'|} \frac{\beta}{R} + (\rho_s - \rho_l) \left( \frac{\Omega^2 R^2}{2} - g\zeta \right) = 0. \quad (25b)$$

We see from Eqs. (23), (25a) that due to rotation there is a general tendency in favor of concave meniscus like Eq. (24), with  $\zeta' > 0$ . On the other hand, near the walls we have  $\zeta' < 0$ . But in this case, in contrast to common situation,  $\zeta'$  cannot just change its sign at some point. Due to the singularity in the first term of Eq. (25a), this change lead to the formation of a facet. Therefore, at sufficiently large  $\Omega$  we have, besides the central one, one more, ring-shaped facet (Fig. 5b).

Let  $\zeta = \zeta_1$  be the level of the initial facet,  $R_1$  be its equilibrium radius. There is a relation between these quantities which can be found by integration of Eq. (25a) over the facet area:

$$R_1 \frac{df}{d\zeta'} \Big|_{R_1+0} + (\rho_s - \rho_l) \left( \frac{\Omega^2 R_1^4}{8} - \frac{gR_1^2}{2} \zeta_1 \right) = 0,$$

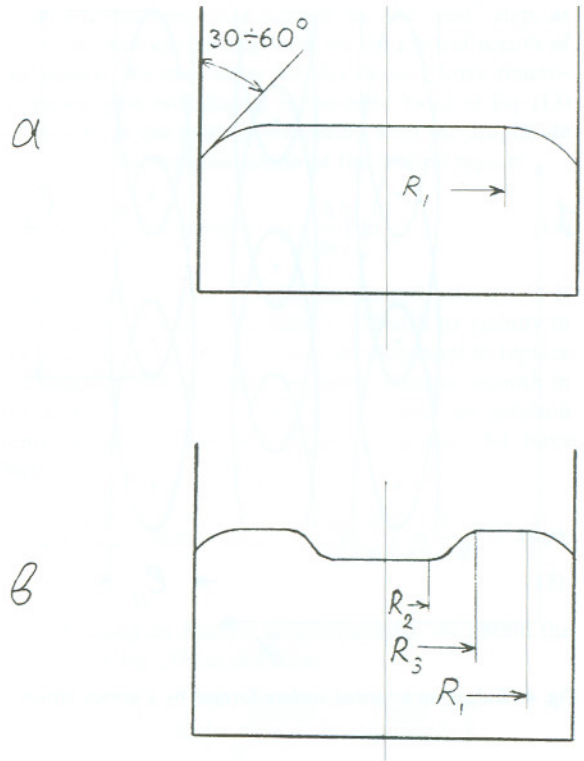


Fig. 5. Splitting of a facet at fast rotation: (a)  $\Omega < \Omega_c$ , (b)  $\Omega > \Omega_c$ .

or, substituting  $(df/d\zeta') \Big|_{R_1+0} = \beta(\zeta'/|\zeta'|) = -\beta$ ,

$$-\frac{\beta}{(\rho_s - \rho_l)} + \frac{\Omega^2 R_1^3}{8} - \frac{gR_1}{2} \zeta_1 = 0. \quad (26)$$

The second facet appears at some angular velocity  $\Omega_c$ , when  $\zeta'$  first change its sign (at some  $R = R_2$ ). It is easy to see that  $R_2 < R_1$ . Indeed, assume for the moment that  $R_2 \geq R_1$ . In this case  $\zeta(R)$  should have an inflection point at  $\bar{R}$ ,  $R_2 \geq \bar{R} \geq R_1$ ,  $\zeta(\bar{R}) = \tilde{\zeta} \leq \zeta_1$ . From Eq. (25b) we have

$$-\frac{\beta}{(\rho_s - \rho_l)} + \frac{\Omega^2 \bar{R}^3}{2} - g\bar{R}\tilde{\zeta} = 0, \quad (27)$$

and, comparing with Eq. (26), we arrive at  $\tilde{\zeta} > \zeta_1$ , in contradiction with our assumptions. So,  $R_2 < R_1$ .

We see that at  $\Omega \geq \Omega_c$  the initial facet splits in two parts with  $\zeta = \zeta_2$ ,  $R < R_2$  and  $\zeta = \zeta_1$ ,  $R_3 < R < R_1$ . Assume that this splitting is a continuous transition, i.e. at  $\Omega = \Omega_c$ ,  $\zeta_2 = \zeta_1$  and  $R_3 = R_2$ . We may write then, similar to Eq. (26) (but the first term is of opposite sign):

$$\frac{\beta}{(\rho_s - \rho_l)} + \frac{\Omega^2 R_2^3}{8} - \frac{gR_2}{2} \zeta_1 = 0. \quad (28)$$



Now, combining Eqs. (26) and (28), we obtain

$$\Omega = \sqrt{\frac{8\beta}{(\rho_s - \rho_l)} \frac{1}{R_1 R_2 (R_1 - R_2)}}. \quad (29)$$

This expression reaches its minimum at  $R_2 = R_1/2$ . We have finally,

$$\Omega_c = \sqrt{\frac{32\beta}{(\rho_s - \rho_l) R_1^3}}. \quad (30)$$

It is necessary to note here that in practice the facet sizes are typically far from their equilibrium values. It means that in real experiments most probably will be observed metastable states of one or another type rather than equilibrium facet.

As for the structures of curved parts of the crystal surface at  $\tau = 0$ , their parameters will be defined by local values of averaged (over  $r \sim b$ )  $\zeta'$ , which play the role of effective tilt angle in this case. These parameters will change very significantly from point to point, the bulges forms become more complicated due to the steps curvature, and only one feature seems to be clear at the moment: the distribution of ridges and terraces will show a hexagonal symmetry in accordance with the symmetry of the vortex lattice.

## 6. Conclusion

We have shown that vortices in rotating superfluid helium form various structures on the liquid–solid helium interface. The sizes of some of these structures seem to be large enough for direct optical observation. Indeed, using modern experimental techniques [4], one can measure a profile of such an interface with the space resolution of the order of 300–500 Å in the  $z$ -direction and 0.02–0.03 mm in the  $x$ – $y$ -plane. From the numerical estimations of the sizes of ridges, given by Eqs. (20), (21), we see that there is a good chance to detect these structures optically at least at sufficiently fast rotation,  $\Omega \sim 1$  rad/s or faster, and low temperatures,  $T \sim 0.1$  K or lower. One also can try to observe the ridges disintegration into separate hillocks, reducing  $\Omega$  and keeping the temperature as low as possible, but such an experiment looks rather difficult. In particular, for successful experiments of this kind extremely low level of mechanical vibrations is needed, due to very high mobilities of vicinal interfaces at low temperatures. Unfortunately hillocks on the basal plane turn out to be too small for optical detection.

As for the observation of the facet splitting at high rotation speeds, it seems to be much easier; at least, in this case there is no need to keep extremely low vibration level and highest space resolution. The most favorable temperatures for this experiment are about

1.1–1.2 K, in the vicinity of the roughening transition temperature  $T_R$ , where the values of  $\beta$  are very small [15] and, as a result, the critical angular velocities  $\Omega_c$  are not too high.

In principle, Eq. (30) could be used for independent determination of  $\beta$  at any temperature below  $T_R$ . However, in such experiments we need true equilibrium conditions as well as when one measures the equilibrium size of a facet (see Refs. [12, 14]). As we already mentioned, typically in real experiments there is no chance to achieve equilibrium facet size. The most realistic explanation of this fact is based on strong asymmetry of the facets kinetics – fast melting and very slow growth. Experiments with rotating crystals provide a new possibility, which was suggested by Rolley. One could try to obtain the value of  $\beta$  from Eq. (26), measuring  $R_1$  and  $\zeta_1$  as functions of  $\Omega$  in the process when  $R_1$  increase,  $\zeta_1$  decrease (the facet melts) with increasing  $\Omega$ . This possibility looks more promising than similar method, when the whole crystal slowly melts without rotation, but such measurements will be very sensitive to mechanical vibrations. Note finally that while using Eq. (26) one should remember that  $\zeta_1$  is measured from a reference level  $z_0$ , that depends on  $\Omega$ . This dependence can be obtained from the condition that the crystal volume remains constant under rotation:

$$V = 2\pi \int_0^{R_0} \zeta^0 R dR = \text{const}. \quad (31)$$

where  $\zeta^0 = \zeta + z_0$ .

The facet height measured from the bottom of the vessel will be  $\zeta_1^0 = \zeta_1 + z_0$ . Now, integrating Eq. (25) over the whole surface and using Eq. (31), we obtain

$$\zeta_1^0 = -\frac{2\beta}{(\rho_s - \rho_l)gR_1} - \frac{\Omega^2}{4g} (R_0^2 - R_1^2) + \text{const}. \quad (32)$$

## Acknowledgements

The author is very grateful to A. Andreev, A. Babkin, R. Bowley, M. Krusius, E. Rolley, E. Sonin, G. Volovik for useful discussions. This work was supported in part by the Academy of Finland and by the Russian Academy of Sciences through the ROTA project.

## References

- [1] K.C. Harvey and A.L. Fetter, *J. Low Temp. Phys.* 11 (1973) 473.
- [2] E.B. Sonin and A.J. Manninen, *Phys. Rev. Lett.* 70 (1993) 2585.

- [3] P.L. Marston and W.M. Fairbank, *Phys. Rev. Lett.* 39 (1977) 1208.
- [4] A.J. Manninen, J.P. Pekola, G.M.Kira, J.P. Ruutu, A.V. Babkin, H. Alles and O.V. Lounasmaa, *Phys. Rev. Lett.* 69 (1992) 2392; see also *Physica B*, this issue.
- [5] O.A. Andreeva, K.O. Keshishev and S.Yu. Osip'yan, *JETP Lett.* 49 (1989) 759.
- [6] E. Rolley, E. Chevalier, C. Guthmann and S. Balibar, *Phys. Rev. Lett.* 72 (1994) 872.
- [7] M.Uwaha and P. Nozières, *J. Physique* 47 (1986) 263.
- [8] M. Kagan, *Sov. Phys. JETP* 63 (1986) 288.
- [9] P. Nozières, in: *Solids Far From Equilibrium*, ed. C. Godrèche (Cambridge Univ. Press, Cambridge, 1991).
- [10] E.Rolley, private communication.
- [11] A.F. Andreev, *JETP Lett.* 52 (1990) 619.
- [12] A.V. Babkin, D.B. Kopeliovich and A.Ya. Parshin, *Sov. Phys. JETP* 62 (1985) 1322.
- [13] W.I. Glaberson and R.J. Donnelly, in: *Progress in Low Temperature Physics*, IX, ed. D.F. Brewer (North-Holland, Amsterdam, 1986).
- [14] K.O. Keshishev, A.Ya. Parshin and A.I. Shalnikov, in: *Soviet Scientific Reviews, Section A: Physics Reviews*, Vol. 4, ed. I.M. Khalatnikov (1982).
- [15] P.E. Wolf, F. Gallet, S. Balibar, E. Rolley and P. Nozières, *J. Physique* 46 (1985) 1987.
- [16] Quite recently Andreev (to be published in *Sov. Phys. JETP*) has shown from energy considerations that in the case of liquid–solid helium interface there is an additional mechanism of the surface instability due to the interaction of steps with moving liquid; however, the axisymmetric solution (8) remains stable even in the presence of this mechanism.